

Boson-Fermion pairing in Bose-Fermi mixtures on 1D optical lattices

X. Barillier-Pertuisel^{1,2} S. Pittel³ L. Pollet⁴ P. Schuck^{1,2,5}

¹*Institut de Physique Nucléaire, IN2P3-CNRS, UMR8608, Orsay, F-91406, France*

²*Université Paris-Sud, F-91406 Orsay, France*

³*Bartol Research Institute and Department of Physics and*

Astronomy, University of Delaware, Newark, Delaware 19716, USA

⁴*Institut Theoretische Physik, ETH Zürich, CH-8093 Zürich, Switzerland*

⁵*Laboratoire de Physique et Modélisation des Milieux Condensés, CNRS Université*

Joseph Fourier, Maison des Magistères, B.P. 166, 38042 Grenoble Cedex 9, France

(Dated: November 7, 2018)

Boson-fermion pairing is considered in a discrete environment of bosons and fully spin-polarized fermions, coupled via an attractive Bose-Fermi Hubbard Hamiltonian in one dimension. The results of the T-matrix approximation for particles of equal mass and at double half filling are compared with the results of exact diagonalization and with Quantum Monte Carlo results. Satisfactory agreement for most quantities is found. The appearance of a stable, weak-coupling pairing mode is also confirmed.

PACS numbers: 03.75.Fi, 05.30.Fk

One of the most intriguing aspects in the field of cold atoms involves the study of mixed Bose-Fermi (B-F) systems. Several boson-fermion mixtures have been realized, both in [1] and without [2] an optical lattice, and their properties have been studied. Several very interesting phenomena unique to mixed BF systems have been predicted, including for example the possibility of forming composite fermions through the pairing of a boson and a fermion [3, 4]. On the theoretical side, B-F mixtures have been studied in mean-field approximation [5, 6] and with various methods for treating B-F mixtures in one dimension (1D). This includes exact solution using the Bethe ansatz [7], bosonization techniques [8] and a Quantum Monte Carlo treatment for a B-F mixture on an optical lattice [9]. There remains, however, the need for theoretical approaches capable of reliably describing B-F mixtures in more than one dimension [10].

A possible theoretical approach to mixed boson-fermion systems was proposed recently in the context of nuclear physics, to provide a framework for describing the transition from a fermi gas (of quarks) to one of composite fermions (nucleons), i.e. bound three-quark states. This problem was simplified by assuming that two of the quarks are strongly bound and form a boson. In this way, the extremely complex in-medium three-body problem [11] was replaced by the much simpler two-body problem of fermion-boson scattering, for which a T matrix approach was developed [12]. An interesting result of that study was that, due to the presence of a Fermi surface, a stable B-F branch was created for an arbitrarily small B-F attraction. The underlying mechanism turned out to be analogous to the formation of stable Cooper pairs in a pure fermi-gas, though in the latter case the pairs are boson-like, whereas here they are fermion-like. Sev-

eral interesting questions follow naturally. On the one hand, we would like to know how reliable the information provided by the T-matrix approach developed in [12] is when dealing with complex systems involving bosons and fermions. If it is found to be acceptably reliable, we might then hope to further develop the method for application to the variety of systems in which boson and fermions degrees of freedom coexist, such as those that arise in cold atomic gases.

As the next step in this program, we report in this work a study of B-F pairing in 1D optical lattices using the above T-matrix approach. Such systems can be treated statistically exactly for a fairly large number of bosons and fermions using Quantum Monte Carlo methods [9], thereby providing an appropriate testing ground for our method. As we will see, even though 1D is a quite unfavorable case for the applicability of a T-matrix approach in ladder approximation, most quantities are nevertheless reproduced reasonably well with this approach over a large range of coupling strengths.

To be more specific, we consider the bosons and fermions on a 1D lattice governed by a Hubbard model hamiltonian. The B-F interaction is assumed to be attractive and the B-B interaction to be repulsive. We assume further that there are no interaction among fermions, although a repulsive F-F interaction should not alter qualitatively our conclusions. The Hubbard model hamiltonian for such a system is given by

$$\mathcal{H} = -t^b \sum_{\langle ij \rangle} b_i^\dagger b_j - t^f \sum_{\langle ij \rangle} c_i^\dagger c_j + \frac{U_{bb}}{2} \sum_i b_i^\dagger b_i^\dagger b_i b_i + U_{bf} \sum_i b_i^\dagger c_i^\dagger c_i b_i, \quad (1)$$

where b_i and c_i are the bosonic and fermionic annihil-

iation operators on site i , respectively. The intersite spacing a is set to unity, i.e. $a = 1$. In this work we carry out our analysis at zero temperature, i.e. $T = 0$. For the QMC simulations, we use a small but finite inverse temperature $\beta = 2L$ which is sufficiently close to the ground state. Extrapolations to larger β do not lead to significantly different results.

In the standard T-matrix approach [13] to this problem, we must solve the Bethe-Salpeter equation for the B-F propagator, that is [12]

$$G_{\mathbf{k},\mathbf{k}'}(\mathbf{K}, E) = G_{\mathbf{k}}^0(\mathbf{K}, E) \delta_{\mathbf{k},\mathbf{k}'} + \sum_{\mathbf{k}_1} G_{\mathbf{k}}^0(\mathbf{K}, E) V_{\mathbf{k},\mathbf{k}_1}^{bf} G_{\mathbf{k}_1,\mathbf{k}'}(\mathbf{K}, E), \quad (2)$$

with $G_{\mathbf{k},\mathbf{k}'}(\mathbf{K}, E)$ being the Fourier transform of the B-F propagator

$$G_{\mathbf{k},\mathbf{k}'}^{t-t'}(\mathbf{K}) = -i\theta(t-t') \left\langle \left\{ \left(b_{\frac{\mathbf{K}}{2}-\mathbf{k}} c_{\frac{\mathbf{K}}{2}+\mathbf{k}} \right)^t, \left(c_{\frac{\mathbf{K}}{2}+\mathbf{k}'}^+ b_{\frac{\mathbf{K}}{2}-\mathbf{k}'}^+ \right)^{t'} \right\} \right\rangle$$

Here $\{, \}$ denotes an anticommutator, \mathbf{K} is the center-of-mass momentum of the pair and \mathbf{k}, \mathbf{k}' are relative momenta. The interactions in momentum space are ($\nu = (bf, bb)$)

$$V_{\mathbf{k},\mathbf{k}'}^\nu = \frac{U_\nu}{L} \delta_{\mathbf{k},\mathbf{k}'} = g_\nu \delta_{\mathbf{k},\mathbf{k}'} \quad (3)$$

and $G_{\mathbf{k}}^0(\mathbf{K}, E)$ is the B-F propagator in the HF approximation, i.e.

$$G_{\mathbf{k}}^0(\mathbf{K}, E) = \frac{\theta(\varepsilon_{\mathbf{k}}^f - \varepsilon_F) + \delta_{\mathbf{K},\mathbf{k}} n_0}{E - \tilde{\varepsilon}_{\mathbf{k}}^f - \tilde{\varepsilon}_{\mathbf{K}-\mathbf{k}}^b + i\eta}, \quad (4)$$

with

$$\tilde{\varepsilon}_{\mathbf{q}}^b = \varepsilon_{\mathbf{q}}^b + \sum_{\mathbf{k}} V_{\mathbf{k}\mathbf{q},\mathbf{k}\mathbf{q}}^{bf} \Theta(\varepsilon_F - \varepsilon_{\mathbf{k}}^f) + 2n_0 V_{\mathbf{q}0,\mathbf{q}0}^{bb},$$

$$\tilde{\varepsilon}_{\mathbf{k}}^f = \varepsilon_{\mathbf{k}}^f + V_{\mathbf{k}0,\mathbf{k}0}^{bf} n_0.$$

In these expressions, n_0 represents the boson condensate, \mathbf{p} (\mathbf{h}) refers to a fermion momentum above (below) the Fermi surface, \mathbf{q} is a boson momentum and $\varepsilon_{\mathbf{k}}^{(f,b)} = -2t^{(f,b)} \cos(\mathbf{k})$. The single particle energies in the denominator of (4) are the fermion and boson HF energies, which are taken together with the unrenormalized interaction, as is usual in the HF-RPA self-consistent scheme [14]. Screening terms which would renormalize on the same footing the interaction and the single particle self energies are not considered in this prototype study but may be included in later work.

Equation (2) can be solved analytically and the propagator summed over relative momenta is given by

$$G(\mathbf{K}, E) = \frac{G^0(\mathbf{K}, E)}{1 - g_{bf} G^0(\mathbf{K}, E)}, \quad (5)$$

with $G(\mathbf{K}, E) = \sum_{\mathbf{k},\mathbf{k}'} G_{\mathbf{k},\mathbf{k}'}(\mathbf{K}, E)$. For a discrete number of sites, it is also useful to consider the equivalent diagonalization problem which can be thought of as a B-F Random Phase Approximation in the particle-particle channel in complete analogy with the pure fermion case [14]. The relevant RPA eigenvalue equation is

$$\begin{pmatrix} \mathcal{A}_{\mathbf{p}'\mathbf{q}',\mathbf{p}\mathbf{q}} & \mathcal{B}_{\mathbf{p}'\mathbf{q}'} \\ \mathcal{B}_{\mathbf{h}'0,\mathbf{p}\mathbf{q},\mathbf{h}0} & \mathcal{C}_{\mathbf{h}'0,\mathbf{h}0} \end{pmatrix} \begin{pmatrix} X_{\mathbf{p}\mathbf{q}}^\alpha & Y_{\mathbf{p}\mathbf{q}}^\rho \\ Y_{\mathbf{h}}^\alpha & X_{\mathbf{h}}^\rho \end{pmatrix} = \begin{pmatrix} X_{\mathbf{p}'\mathbf{q}'}^\alpha & Y_{\mathbf{p}'\mathbf{q}'}^\rho \\ Y_{\mathbf{h}'}^\alpha & X_{\mathbf{h}'}^\rho \end{pmatrix} \begin{pmatrix} E_\alpha & 0 \\ 0 & -E_\rho \end{pmatrix}, \quad (6)$$

$$\mathcal{A}_{\mathbf{p}'\mathbf{q}',\mathbf{p}\mathbf{q}} = \delta_{\mathbf{p}\mathbf{p}'} \delta_{\mathbf{q}\mathbf{q}'} (\tilde{\varepsilon}_{\mathbf{p}}^f + \tilde{\varepsilon}_{\mathbf{q}}^b) + a(\mathbf{q}) V_{\mathbf{p}'\mathbf{q}',\mathbf{p}\mathbf{q}}^{bf} a(\mathbf{q}'),$$

$$\mathcal{B}_{\mathbf{h}'0,\mathbf{p}\mathbf{q}} = V_{\mathbf{h}'0,\mathbf{p}\mathbf{q}}^{bf} \sqrt{n_0} a(\mathbf{q}),$$

$$\mathcal{B}_{\mathbf{p}'\mathbf{q}',\mathbf{h}0} = V_{\mathbf{p}'\mathbf{q}',\mathbf{h}0}^{bf} \sqrt{n_0} a(\mathbf{q}'),$$

$$\mathcal{C}_{\mathbf{h}'0,\mathbf{h}0} = \delta_{\mathbf{h}\mathbf{h}'} (\tilde{\varepsilon}_{\mathbf{h}}^f + \tilde{\varepsilon}_{\mathbf{h}}^b) + \delta_{\mathbf{h}\mathbf{h}'} V_{\mathbf{h}0,\mathbf{h}0}^{bf} n_0,$$

where we define $a(\mathbf{q}) = \sqrt{1 + \delta_{\mathbf{q},0} n_0}$ and $V_{\mathbf{p}\mathbf{q},\mathbf{p}'\mathbf{q}'}^\nu = g_\nu \delta_{\mathbf{p}+\mathbf{q},\mathbf{p}'+\mathbf{q}'}$. In terms of the amplitudes X, Y the propagator (3) can be written in the following spectral representation:

$$G_{\mathbf{k},\mathbf{k}'}(\mathbf{K}, E) = \sum_{\alpha} \frac{\chi_{\mathbf{k}}^\alpha \chi_{\mathbf{k}'}^{\alpha+}}{E - E_\alpha} + \sum_{\rho} \frac{\chi_{\mathbf{k}}^\rho \chi_{\mathbf{k}'}^{\rho+}}{E + E_\rho}, \quad (7)$$

with $\chi_{\mathbf{k}}^{\alpha+} = (Y_{\mathbf{k}}^\alpha X_{\mathbf{k},\mathbf{K}-\mathbf{k}}^\alpha)$ and $\chi_{\mathbf{k}}^{\rho+} = (Y_{\mathbf{k},\mathbf{K}-\mathbf{k}}^\rho X_{\mathbf{k}}^\rho)$. For a system with N particles, the propagator has poles at $E_{\rho,\alpha} = \pm(E_0^N - E_{\rho,\alpha}^{N\pm 2})$, i.e. essentially at the excitation energies of the $N \pm 2$ systems. The RPA amplitudes obey the following normalization conditions:

$$Y_{\mathbf{K}}^\alpha Y_{\mathbf{K}}^{\alpha'} \Theta(\varepsilon_F - \varepsilon_{\mathbf{K}}^f) + \sum_{\mathbf{p}} X_{\mathbf{p},\mathbf{K}-\mathbf{p}}^\alpha X_{\mathbf{p},\mathbf{K}-\mathbf{p}}^{\alpha'} = \delta_{\alpha\alpha'},$$

$$X_{\mathbf{K}}^\rho X_{\mathbf{K}}^{\rho'} \Theta(\varepsilon_F - \varepsilon_{\mathbf{K}}^f) + \sum_{\mathbf{p}} Y_{\mathbf{p},\mathbf{K}-\mathbf{p}}^\rho Y_{\mathbf{p},\mathbf{K}-\mathbf{p}}^{\rho'} = \delta_{\rho\rho'} \quad (8)$$

To assess the quality of our T-matrix approximation for the in-medium B-F problem, we consider finite numbers of sites, where exact solution is possible. We first restrict to half-filling and to $N_B = N_F$ and $t_b = t_f$. We exactly diagonalize the 6-site problem, i.e. $N_B = N_F = 3$. The maximum size of the matrix is 318×318 , whereas the RPA matrix has dimension 4×4 . The range of U_{bf} values is arbitrary. However, since we are interested in B-F pairing, the range of U_{bb} values is, in principle, restricted to $U_{bb} \geq |U_{bf}|/2$. Smaller values of U_{bb} lead to phase separation, i.e. the B-F pairs cluster together and occupy only half of the available space [9]. On the other hand, our T-matrix approximation does not allow U_{bb} -values greater than $U_{bb} \simeq |U_{bf}|$, since U_{bb} is only purely treated in our theory, i.e. only in HF approximation. Improving on

this point is possible but left for the future. We therefore limit ourselves to $|U_{bf}| \geq U_{bb} \geq |U_{bf}|/2$. As an intermediate value we take $U_{bb} = \frac{3}{4}|U_{bf}|$ throughout.

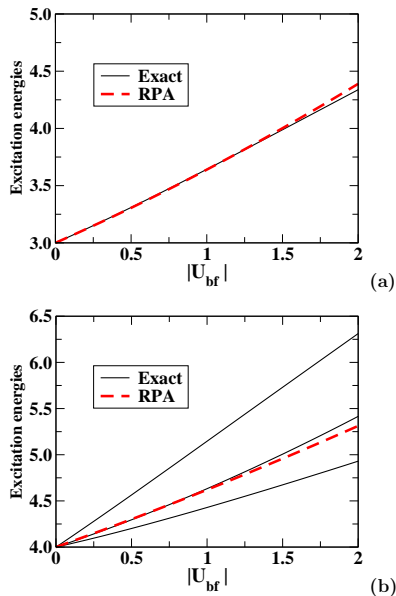


FIG. 1: (Color online) Excitation energy as a function of $|U_{bf}|$ for the 6-site B-F Hubbard model and $\mathbf{K} = \pi/3$ (a) and for $\mathbf{K} = 0$ (b). The solid lines correspond to the results of exact diagonalization and the dashed lines to the RPA results.

In Fig. 1, we present some typical examples of excited states. We see that the agreement between approximate and exact excitation energies is quite satisfactory. We should note that we have chosen examples where in the exact case there are only low degeneracies at $U_{bf} = 0$, since RPA, because of its very low dimension, can not well reproduce a high degeneracy of uncorrelated configurations, even if there are also cases in RPA where in the uncorrelated limit degeneracies occur. However these degeneracies are always less numerous than in the exact case. This is natural because of the dramatically reduced size of the RPA matrices with respect to the size of the exact ones. It should nevertheless be noted that the RPA excitation energies somehow represents the average trend of the bunch of exact levels.

So far we have not invested effort to exactly diagonalize problems with higher numbers of sites, since the dimensions of the matrices grow exponentially. However, exact QMC results for ground state properties for higher number of sites are available [9]. For $L = 70$ we show a comparison of the exact ground state energy E_0 with the RPA in Fig. 2 (see [12] for the expression for E_0). The error bars for QMC are smaller than the point size. Again the agreement is reasonable up to rather high values of $|U_{bf}|$.

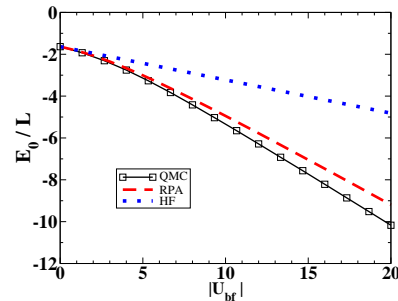


FIG. 2: (Color online) Ground state energy per site as a function of $|U_{bf}|$ for $L = 70$. The solid line corresponds to the QMC, dotted line to the HF approximation and dashed line to the RPA.

We also calculated the occupation numbers $n_{bf}(\mathbf{K}) = \sum_{\mathbf{k}\mathbf{k}'} \langle c_{\mathbf{K}-\mathbf{k}}^+ b_{\mathbf{k}}^+ b_{\mathbf{k}'} c_{\mathbf{K}-\mathbf{k}'} \rangle$ of the B-F pairs and compare them with the exact results in Fig. 3a. In our case the B-F occupation numbers are simply obtained from the residue of the B-F Green's function (5) at the poles E_ρ . We see that the agreement with the exact result is quite satisfactory. One might wonder about the upward tendency around $\mathbf{K} = \pi/2$ in the BF occupation numbers for the RPA data, since it is much more pronounced than in the QMC data. Notice, however, that for other system parameters the upward trend in the occupation numbers can also be quite pronounced even in the exact solution. Probably, the RPA gives relatively more weight to the density wave correlator than to the superfluid properties because of the truncated model space and the fact that in three dimensions a gapped density wave was found in DMFT [15].

The fermion occupation numbers $n_f(\mathbf{k}) = \langle c_{\mathbf{k}}^+ c_{\mathbf{k}} \rangle$ can only be obtained in a somewhat indirect way within our formalism. This goes, however, completely parallel to what is known from the usual RPA formalism for fermions [16]. The corresponding expression is given by

$$n_f(\mathbf{k}) = \sum_{\rho} |X_{\mathbf{k}}^{\rho}|^2 \Theta(\varepsilon_F - \varepsilon_{\mathbf{k}}^f) + \sum_{\mathbf{K}, \rho} |Y_{\mathbf{k}, \mathbf{K}-\mathbf{k}}^{\rho}|^2 \Theta(\varepsilon_{\mathbf{k}}^f - \varepsilon_F) \quad (9)$$

One can demonstrate that (9) conserves fermion particle number. In Fig. 3b the fermion occupation numbers are shown for two cases of the coupling $U_{bf} = -2, -6$. Again the agreement with the exact case is rather good, in spite of the fact that for $U_{bf} = -6$ our solution shows a small Fermi step whereas the exact one seems to be completely smooth. One should realize, however, that our theory can not describe a non-Fermi liquid behavior and this seems to be the case for stronger interactions in the exact solution. This deficiency of our approach to describe specific 1D features shows up more dramatically for the boson occupation numbers where we still obtain a large fraction

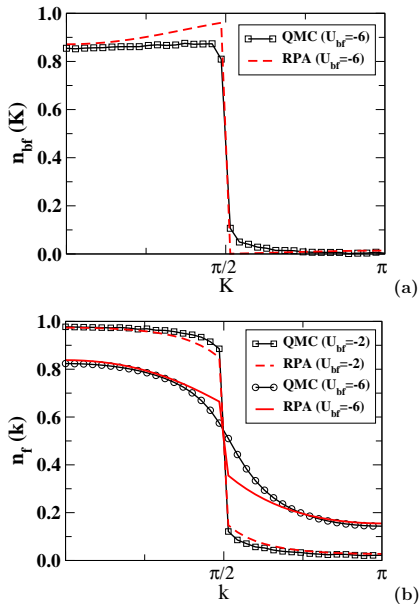


FIG. 3: (Color online) (a)BF occupation numbers as a function of the total momentum \mathbf{K} , and (b)Fermion occupation numbers as a function of the relative momentum \mathbf{k} ($U_{bb} = 0.75|U_{bf}|$, $L = 70$).

of particles condensed into the $\mathbf{q} = 0$ state whereas the exact solution is, of course, totally distributed with no particles in the condensate. In spite of this failure, we conclude, however, that our first objective of the work has been realized, namely our T-matrix approach which has been applied for the first time to the in-medium B-F case in [12] seems to work reasonably well. In addition, for $t_b \neq t_f$, our formalism is still valid. We compare in Table I the ground-state energies obtained by RPA, HF, and QMC for $t_f = 4t_b$, and see that the results are still of the same quality as for the case with equal tunneling amplitude (see Fig. 2). Similar conclusions hold for the occupation numbers and for a comparison with exact diagonalization for a system size $L = 6$. We also should note that we even-

$(U_{bf}; U_{bb})$	E_{RPA}	E_{HF}	E_{QMC}
(-40;6)	-24.30	-12.85	-20.78
(-50;10)	-29.71	-14.88	-25.54
(-60;12)	-35.69	-17.15	-30.33

TABLE I: Comparison of the ground state energies per site obtained by RPA, HF and QMC for a system of size $L = 30$ and tunneling amplitudes $t_f = 4t_b$. The HF and RPA relative errors are roughly constant.

tually would like to apply our theory to the 3D case where mean field and RPA theories usually perform much better, and where no QMC data are available.

Another objective of this work is to confirm a surprising finding discussed in [12], the appearance of

a second stable B-F branch at arbitrary small B-F (attractive) interaction. It exists only because of the presence of a sharp Fermi surface and is thus analogous to the formation of Cooper pairs in pure Fermi systems. For this investigation, we pass to the continuum limit in which the B-F propagator in HF approximation is given analytically by

$$G_K^0(E) = \frac{x}{\pi L P^0} \frac{1}{\sqrt{x^2 - 1}} \left(\arctan \left(\frac{(x+1) \cot(\frac{K}{4} + \frac{k_f}{2})}{\sqrt{x^2 - 1}} \right) - \arctan \left(\frac{(x+1) \cot(\frac{k_f}{2} - \frac{K}{4})}{\sqrt{x^2 - 1}} \right) \right) + \frac{n_0/L}{P^1 + 2 + 2 \cos(K)},$$

with

$$x = \frac{P^0}{4 \cos(\frac{K}{2})},$$

$$P^0 = E + \frac{2k_f}{\pi} (U^{bb} + U^{bf}) + i\eta,$$

$$P^1 = E + \frac{k_f}{\pi} (U^{bb} + U^{bf}) + i\eta.$$

In Fig.4 we show the spectral function, i.e. $-Im(G(K, E))/\pi$, for a typical set of parameters for $N_B = N_F = L/4$, away from half filling. Besides the low lying peak which corresponds to the free fermion dispersion in the $U_{bf} \rightarrow 0$ limit, we see the striking feature that a second stable branch develops right below the continuum. This stable second branch exists for arbitrarily small values of U_{bf} . It is the same phenomenon as was seen in our earlier work [12]. The existence of a Fermi surface entails a logarithmic divergence of $Re(G^0)$ at $E/2 = \varepsilon_F$ and then there is always a sharp state below the continuum solution of $1 - g_{bf} G^0(\mathbf{K}, E) = 0$. However contrary to what happens in the homogeneous continuum case [12], this second branch does not interact strongly with the lowest free fermion-like branch. In [12] there was a level crossing of the two branches which does not occur here. Also the upper branch has rather little spectral weight compared with the lower one. It would be interesting to see whether this second branch can be found experimentally. In 1D, however, we should note that this slightly detached second branch is certainly an artefact of the T-matrix approximation because the correlated fermion occupation numbers do not show any discontinuity (see fig. 3). However in 2D or 3D, we think that this second branch should exist. Whether it survives in a trap geometry [17] remains to be seen.

In conclusion, we have investigated in this work boson-fermion pairing in a Bose-Fermi mixture on a 1D optical lattice. The in-medium Boson-Fermion scattering problem was solved in T-matrix approximation. As in a previous investigation, in the thermodynamical limit, two stable branches were

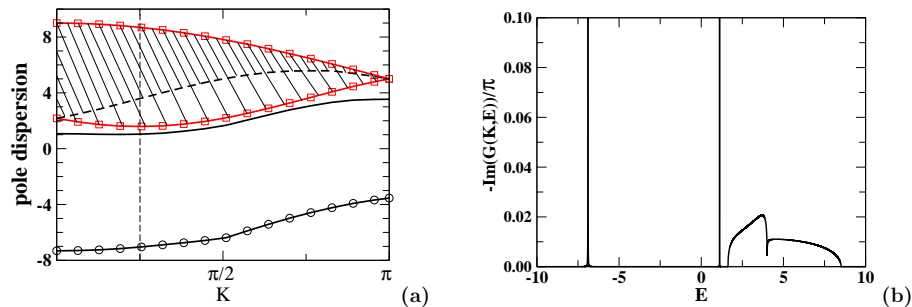


FIG. 4: (Color online) (a) The solid line with circles represents the free fermion-like branch of the spectral function, the solid line the second B-F branch, the solid lines with squares the limits of the continuum and the dashed line a second plateau in the continuum, (b) The spectral representation corresponding to (5) for $\mathbf{K} = \pi/4$, see vertical broken line of (a) ($U_{bf} = -10$, $k_F = \pi/4$).

found. One corresponds to the elastic scattering of the fermions off the Bose condensate and the other is created from scattering of bosons out of the condensate with fermions above the Fermi sea. The latter comes because of the presence of a sharp Fermi surface and therefore has the same origin as the Cooper pole in a pure two component Fermi system. While in 1D systems, the second branch is unphysical and just an artefact of the method, we think that in 3D such a branch should be real. We checked the validity of our approach versus exact results available for a finite number of sites. For most quantities we found good qualitative and semi-quantitative agreement. This is satisfying because, as already

mentioned, RPA generally works better in higher dimensions. More elaborate studies of B-F pairing are under way.

Ongoing collaboration and discussions with T. Suzuki and C. Martin on B-F correlations are appreciated. We gratefully acknowledge contributions by J. Dukelsky during the early stages of this work, the financial support of the Swiss National Science Foundation and the partial support of the US National Science Foundation under grant # 0553127. Part of the calculations discussed in this work were carried out on the Hreidar cluster at ETH Zurich.

-
- [1] K. Günter *et al.*, Phys. Rev. Lett. **96**, 180402 (2006); S. Ospelkaus *et al.*, Phys. Rev. Lett. **96**, 180403 (2006).
 - [2] A. G. Truscott *et al.*, Science **291**, 2570 (2001); Z. Hadzibabic *et al.* Phys. Rev. Lett. **91**, 160401 (2003); G. Roati *et al.*, Phys. Rev. Lett. **89**, 150403 (2002).
 - [3] A. B. Kuklov and B. V. Svistunov, Phys. Rev. Lett. **90**, 100401 (2003).
 - [4] M. Lewenstein, L. Santos, M. A. Baranov and H. Fehrmann, Phys. Rev. Lett. **92**, 050401 (2004).
 - [5] A. Albus, F. Illuminati and J. Eisert, Phys. Rev. A **68**, 023606 (2003).
 - [6] H. Fehrmann, M. A. Baranov, B. Danksi, M. Lewenstein and L. Santos, Optics Communications **243**, 23 (2004).
 - [7] A. Imambekov and E. Demler, Phys. Rev. A **73**, 021602 (2006)
 - [8] L. Mathey *et al.*, Phys. Rev. Lett. **93**, 120404 (2004); L. Mathey Phys. Rev. B **75**, 144510 (2007).
 - [9] L. Pollet, M. Troyer, K. Van Houcke and S. M. A. Rombouts, Phys. Rev. Lett. **96**, 190402 (2006).
 - [10] H.P. Büchler and G. Blatter, Phys. Rev. Lett. **91**, 130404 (2003).
 - [11] A. Rapp, G. Zaránd, C. Honerkamp and W. Hofstetter, Phys. Rev. Lett. **98**, 160405 (2007).
 - [12] A. Storozhenko, P. Schuck, T. Suzuki, H. Yabu, J. Dukelsky, Phys. Rev. A **71**, 063617 (2005).
 - [13] A.L. Fetter, J. D. Walecka, *Quantum Theory of Many-Particle Systems* (McGraw-Hill, New York, 1971).
 - [14] P. Ring, P. Schuck, *The Nuclear Many Body Problem* (Springer, New York, 1980).
 - [15] I. Titvinidze, M. Snoek, W. Hofstetter, cond-mat/0708.3241 (2007)
 - [16] A. Bouyssy, N. Vinh Mau, Nucl. Phys. A **229** (1974).
 - [17] L. Pollet, C. Kollath, U. Schollwoeck, M. Troyer, cond-mat/0609604 (2006)